International Journal of Heat and Mass Transfer 78 (2014) 796–804

Contents lists available at ScienceDirect

International Journal of Heat and Mass Transfer

journal homepage: www.elsevier.com/locate/ijhmt

Lattice Boltzmann method for rarefied channel flows with heat transfer

Seckin Gokaltun [a,*], George S. Dulikravich [b]

[a] Applied Research Center, Florida International University, 10555 W Flagler ST EC2100, Miami, FL 33174, USA
[b] Department of Mechanical and Materials Engineering, Florida International University, 10555 W Flagler ST EC3462, Miami, FL 33174, USA

ARTICLE INFO

Article history:
Received 7 October 2013
Received in revised form 6 July 2014
Accepted 8 July 2014
Available online 6 August 2014

Keywords:
Lattice Boltzmann equation
Non-continuum
Microchannel
Convection heat transfer

ABSTRACT

A thermal lattice Boltzmann method (TLBM) is presented for the analysis of fluid flow and heat transfer in two-dimensional channels with non-continuum effects. The relaxation times (τ_f, τ_g) are linked to the Knudsen number which accounts for the rarefaction that can be present at micro geometries or at low density conditions. The TLBM used here employs inlet/outlet boundary conditions to generate a forced convection problem where the calculation of equilibrium distributions at the wall surfaces are modified to incorporate the velocity slip and temperature jump conditions. Numerical simulations are obtained for thermal micro-Couette and thermal micro-Poiseuille channel flows and the effect of the Knudsen number on the velocity and temperature profile is investigated.

1. Introduction

The lattice Boltzmann method is a kinetic method based on the particle distribution function and during the past few years it has gained the attention of many researchers whom investigated the applicability of LBM for simulation of microscale flows (Table 1).

Nie et al. [1] applied the LBM method for compressible flow in microchannels and micro-cavities and they have observed that LBM can capture behaviors such as velocity slip, nonlinear pressure distribution along the channel and dependence of mass flow rate on Knudsen number. In their study they have used a D2Q9 model on a two-dimensional, square lattice. They used a modified relaxation time in order to include the dependence of viscosity on density for compressible flows. They defined the mean free path as a function of viscosity and density multiplied with a coefficient that was determined by comparing simulation results with microchannel experiments. Bounce-back wall boundary conditions were used for the particle distribution functions at the top and bottom plates. This boundary condition results in a non-slip velocity in the continuum regime; however, the results have shown that when *Kn* is large, a mean slip velocity on wall boundary can be achieved. This was owed to the kinetic nature of the LBM.

Lim et al. [2] used specular reflection and a second order extrapolation scheme for gas interaction with surfaces in their LBM simulations. The non-linear pressure distribution, increase of slip velocity along the channel, and radial velocity profile obtained were in agreement with analytical results [3]. Their result for the slip flow regime was in good agreement with experimental data of Pong et al. [4] for pressure distribution along the microchannel. However, it was observed that using different boundary treatment has little influence on pressure distribution, though the effect on slip velocity on the wall surfaces is significant. Further investigation has shown that the mass flow rate and the overall average velocity were in perfect agreement with Arkilic's analytical solution [3] and the mass flow rate was found to be insensitive to the boundary treatment on the wall surfaces.

Tang et al. [5] has combined the bounce-back boundary condition [1] with the specular reflection boundary condition [6] in order to accurately capture the momentum exchange and friction drag between the wall surface and the gas in microflows. They have defined a reflection coefficient r_b for which $r_b = 1$ corresponds to pure bounce-back reflection and $r_b = 0$ to pure specular reflection. Using a value of $r_b = 0.7$ they have successfully matched the mass flow rate and the non-linear pressure variation observed in the experiments by Shih et al. [7] for $Kn = 0.16$. Recently, the authors extended their model to 3D by using a *D*3Q15 lattice model [8]. Their LBM results for nonlinear pressure profiles were in good agreement with the 3D analytical model of Aubert et al. [9].

Shen et al. [10] has extended the work of Nie et al. [1] and compared the results for velocity and pressure distributions for microchannels with the results obtained with DSMC, IP, and slip NS methods. In their LBM simulations they have used bounce-back boundary condition on the walls and the extrapolation scheme [11] at the inlet and exit of the channel. In their definition of the mean free path, they use a coefficient whose value ($a = 0.388$) is

* Corresponding author.
E-mail address: gokaltun@fiu.edu (S. Gokaltun).

http://dx.doi.org/10.1016/j.ijheatmasstransfer.2014.07.018
0017-9310/

Table 1
Lattice Boltzmann method for gas flow in microchannels in literature.

#	Author	Year	*Kn*	Boundary condition
1	Nie et al. [1]	2002	$Kn = \alpha\tau/\rho H$	Bounce back
2	Lim et al. [2]	2002	$Kn = \delta x(\tau + 0.5)/H(P_o/P)$	Specular reflection and extrapolation scheme
3	Tang et al. [5]	2003	$Kn = \alpha\tau/\rho H$	
4	Shen et al. [10]	2004	$Kn = \alpha\tau/\rho H$	Bounce back
5	Lee et al. [12]	2005	$Kn = \delta x\tau/H(P_o/P)$	Wall equilibrium
6	Zhang et al. [15]	2005	$Kn = \alpha\tau/\rho H$	Maxwellian scattering
7	Zhou et al. [20]	2006	$Kn = \alpha\tau/\rho H$	Bounce back

determined from the best match of the results with the experiments. The flow rate prediction of LBM was observed to be in good agreement with other methods for $Kn = 0.0194, 0.194$, and 0.388. The velocity profile and the pressure distribution results were found to be in good agreement with the results of other methods for $Kn = 0.0194$ however for $Kn = 0.194$ and 0.388 the LBM velocity profile and pressure variation were observed to deviate from the results of DSMC and IP. Depending on these results the authors have concluded that the version of LBM proposed by Nie et al. [1] shows feasibility to simulate MEMS gas flow in continuum and slip flow regimes but not in the transition regime where the Knudsen number is large.

Lee et al. [12] proposed a second order definition of Knudsen number and a wall equilibrium boundary condition for LBM to simulate gas flows in a microchannel. They tested their method for gas flow in a periodic microchannel with constant external pressure gradient. The normalized slip velocity was found to be in excellent agreement with the analytical prediction of Arkilic [3] for $Kn < 0.1$. They validated their proposed LBM method by comparing their results for normalized streamwise velocity profile with those of the linearized Boltzmann equation [13] and the DSMC methods [14] for $Kn = 0.1$. The LBM solution was found to be in excellent agreement with the others. Their model was also tested for gas flow in a microchannel with constant pressures at inlet and exit. It was shown that the slip velocity is in good agreement with Arkilic's prediction [3]. They have concluded that their proposed method for the definition of Knudsen number and the wall equilibrium boundary condition is more physically meaningful compared to previous versions of LBM simulations for microchannel flow [1,2].

Zhang et al. [15] showed that LBM can predict the correct trend of mass flow rate as the Knudsen number increases along the microchannel and captures the "Knudsen minimum" phenomena, which was observed previously in experiments [16]. A slip boundary condition was proposed by adopting the Maxwellian scattering kernel to describe gas surface interactions. Their proposed boundary condition requires the assignment of a constant for the accommodation coefficient.

The Knudsen paradox was also captured by Toschi and Succi [17] for flow in a rectangular duct where the flow was driven by a volumetric force along the streamwise direction. In their simulations they compared the performance of the bounce back boundary condition [11] and the kinetic boundary condition proposed by Ansumali and Karlin [18] in the rarefaction range $10^{-3} < Kn < 30$ and at a fixed Mach number $Ma = 0.03$. Being independent from the boundary condition at the wall surfaces, Toschi and Succi have proposed that every LBM simulation at finite *Kn* regime should take care of the momentum transfer along the direction orthogonal to the boundaries. In order to achieve this, they proposed a virtual wall collision (VWC) model that should be implemented at every lattice site in the flow domain. Their simulations have shown that with VWC model the results for the mass flux was in good agreement with the analytical prediction of Cercignani [19]. The bounce back boundary condition has shown to be incapable of predicting the correct wall slip velocity in the high Knudsen number regime. They have concluded that the LBM method using the kinetic wall boundary conditions of Ansumali and Karlin [18] combined with their VWC method [17] can capture continuum and non-continuum effects of microchannel flow.

Lattice Boltzmann method has been introduced to the scientific community as a new alternative numerical method that can solve for flows with complex physics [21,22] however there are still areas that need to be studied in order to obtain a well-established numerical method that covers a wide range of engineering applications. One aspect of this improvement is the solution of flows with heat transfer [23,24]. In an effort to obtain a thermal lattice Boltzmann method (TLBM), a variety of techniques were proposed in the literature, namely the multi-speed approach, the passive-scalar approach and the double populations approach. The model developed by He et al. [25] has gained the most popularity because it was more stable and it had the capability to solve for viscous dissipation and compression work. In this model, the thermal lattice Boltzmann equation was derived by discretizing the Boltzmann equation for the internal energy distribution. As a result, thermal energy and heat flux were able to be obtained by taking the kinetic moments of the thermal energy distribution function.

The method proposed by He et al. [25] was accepted by many researchers and it was successfully applied to solve for various kinds of fluid flow problems with heat transfer. Dixit and Babu [26] used this model to simulate natural convection of a Boussinesq fluid in a square cavity. It was demonstrated that for high Rayleigh numbers the TLBM results agreed well with other benchmark numerical simulations. Tang et al. [27] proposed boundary conditions to improve the same model in order to solve for two-dimensional Poiseuille and Couette flow and verified the TLBM results with Finite Volume Method and analytical solutions at various wall boundary conditions. D'Orazio and Succi [28] introduced a counter-slip internal energy boundary condition for the TLBM model and obtained satisfactory results for hydrodynamically and thermally developed channel flows heated at the inlet. In their simulations, the TLBM was able to capture the effect of viscous dissipation which was tested for thermal Couette flow at various Brinkmann numbers.

There have been a couple of studies that aimed to implement the TLBM in fluid flow and heat transfer in complex geometries. Huang et al. [29] solved the natural convection in a concentric annulus involving circular solid boundaries. The curved non-slip wall boundary treatment for isothermal LBM [30] was extended to treat the thermal curved solid boundary in the two-population TLBM computations. Chen et al. [31] applied the same boundary condition for two-dimensional solutions of backward-facing step flows with inclined plates positioned along the flow field at various angles. Gokaltun and Dulikravich [32] verified the TLBM solutions for a constricted channel flow against FEM solutions for velocity and thermal fields.

Heat transfer in microscales is a major issue in analysis and design of computer chips and cooling of electronic equipments. Due to its kinetic nature, LBM can be an important tool in the study

of the mechanism of microlevel flow and heat transfer. It was shown that thermal LBM successfully predicts heat transfer characteristics in the continuum regime [32] and it has been lately the interest of the academic society to investigate whether it can be further used for micro flow and heat transfer.

Shu et al. [33] have proposed to extend the thermal LBM developed by He et al. [25] to simulate micro flows with heat transfer. They have used a diffuse scattering boundary condition to consider the velocity slip and temperature jump at wall boundaries. The slip length and temperature jump on the wall obtained from their simulations were well agreed with DSMC and analytical data for thermal Couette and thermal developing channel flow. In a later study by the same authors [34], it was shown that the TLBM was able to predict the decrease in local friction coefficient and Nusselt number by increasing the Knudsen number. They further investigated in another study the effect of aspect ratio of the microchannel by using a 3D TLBM solver.

Wang and Yang [35] used TLBM to solve for heat transfer characteristics of fluid flow in a microchannel. They used the bounce-back boundary condition to treat the wall boundaries in their simulations and they were able to obtain slip flow on the solid surfaces. However, the physical explanation of the boundary treatment is not clear and the paper in general cannot be considered as a fine example of TLBM on microflows.

Tian et al. [36] on the other hand, obtained good results with the TLBM for micro-Couette flow with a temperature gradient in the slip flow regime. Their method used Maxwell's first-order slip boundary condition for wall velocity and temperature jump. They were able to show the effect of viscous heat dissipation and heat transfer in microflows.

In the present study, Maxwell's approach is followed for a perfectly diffusive wall boundary. The TLBM is used to simulate micro-Couette flow as well as thermally developing channel flow. The variation of slip velocity and temperature jump can be obtained with the current application of TLBM.

2. Numerical method

In this paper, He's thermal lattice Boltzmann model [25] is adopted to solve for the heat transfer in channel flows. The TLBM solves the following discrete evolution equations:

$$\tilde{f}_a(\mathbf{x}+\mathbf{e_a}\Delta t, t+\Delta t) = \tilde{f}_a(\mathbf{x},t) - \frac{\Delta t}{\tau_p + 0.5\Delta t}\left(\tilde{f}_a(\mathbf{x},t) - f_a^{eq}(\mathbf{x},t)\right), \quad (1)$$

$$\tilde{g}_a(\mathbf{x}+\mathbf{e_a}\Delta t, t+\Delta t) = \tilde{g}_a(\mathbf{x},t) - \frac{\Delta t}{\tau_g + 0.5\Delta t}\left(\tilde{g}_a(\mathbf{x},t) - g_a^{eq}(\mathbf{x},t)\right) - \frac{\tau_g \Delta t}{\tau_g + 0.5\Delta t} f_a(\mathbf{x},t) h_a(\mathbf{x},t). \quad (2)$$

where

$$\tilde{f}_a(\mathbf{x},t) = f_a(\mathbf{x},t) - \frac{\Delta t}{2\tau_p}\left(f_a^{eq}(\mathbf{x},t) - f_a(\mathbf{x},t)\right), \quad (3)$$

$$\tilde{g}_a(\mathbf{x},t) = g_a(\mathbf{x},t) - \frac{\Delta t}{2\tau_g}\left(g_a^{eq}(\mathbf{x},t) - g_a(\mathbf{x},t)\right) + \frac{\Delta t}{2} f_a(\mathbf{x},t) h_a(\mathbf{x},t). \quad (4)$$

In Eq. (4), the term h_a represents the effect of viscous heating and can be expressed as

$$h_a(\mathbf{x},t) = (\mathbf{e_a} - \mathbf{u}) \cdot \left[-\nabla\left(\frac{P}{\rho}\right) + \frac{1}{\rho}\nabla\cdot\Pi + (\mathbf{e_a} - \mathbf{u})\cdot\nabla\mathbf{u}\right], \quad (5)$$

which can be reduced to [27]

$$h_a(\mathbf{x},t) = (\mathbf{e_a} - \mathbf{u}) \cdot [\partial_t \mathbf{u} + (\mathbf{e}\cdot\nabla)\mathbf{u}]. \quad (6)$$

In D'Orazio et al. [24], Eq. (6) is given as:

$$h_a(\mathbf{x},t) = (\mathbf{e_a} - \mathbf{u}(\mathbf{x},t)) \cdot [\mathbf{u}(\mathbf{x}+\mathbf{e_a}\Delta t, t+\Delta t) - \mathbf{u}(\mathbf{x},t)]/\Delta t, \quad (7)$$

which is used in this work to calculate h_a. The new distribution variables $\tilde{f}$ and $\tilde{g}$ are related to old variables f and g as given below:

$$\tilde{f}_a = f_a + \frac{0.5\Delta t}{\tau_p}(f_a - f_a^{eq}), \quad (8)$$

$$\tilde{g}_a = g_a + \frac{0.5\Delta t}{\tau_g}(g_a - g_a^{eq}) + \frac{\Delta t}{2} f_a h_a. \quad (9)$$

The equilibrium density distribution functions for f and g are given as follows:

$$f_a^{eq} = w_a \rho\left[1 + 3\frac{\mathbf{e}_a\cdot\mathbf{u}}{c^2} + \frac{9}{2}\frac{(\mathbf{e}_a\cdot\mathbf{u})^2}{c^4} - \frac{3}{2}\frac{\mathbf{u^2}}{c^2}\right], \quad (10)$$

$$g_{1-4}^{eq} = w_{1-4}\rho e(\mathbf{x})\left[\frac{3}{2} + \frac{3}{2}\frac{\mathbf{e}_a\cdot\mathbf{u}}{c^2} + \frac{9}{2}\frac{(\mathbf{e}_a\cdot\mathbf{u})^2}{c^4} - \frac{3}{2}\frac{\mathbf{u^2}}{c^2}\right], \quad (11)$$

$$g_{5-8}^{eq} = w_{5-8}\rho e(\mathbf{x})\left[3 + 6\frac{\mathbf{e}_a\cdot\mathbf{u}}{c^2} + \frac{9}{2}\frac{(\mathbf{e}_a\cdot\mathbf{u})^2}{c^4} - \frac{3}{2}\frac{\mathbf{u^2}}{c^2}\right], \quad (12)$$

$$g_9^{eq} = w_9\rho e(\mathbf{x})\left[-\frac{3}{2}\frac{\mathbf{u^2}}{c^2}\right]. \quad (13)$$

The weighting coefficients in Eqs. (10)–(13) are selected as $w_{1-4} = 1/9, w_{5-8} = 1/36$ and $w_9 = 4/9$. The D2Q9 lattice structure used in this study is shown in Fig. 1, where particles move along 9 specific directions with speed

$$\mathbf{e_a} = \begin{cases} (\cos[(a-1)\frac{\pi}{2}], \sin[(a-1)\frac{\pi}{2}])c, & a = 1-4, \\ (\cos[(a-5)\frac{\pi}{2} + \frac{\pi}{4}], \sin[(a-5)\frac{\pi}{2} + \frac{\pi}{4}])c, & a = 5-8, \\ (0,0), & a = 9. \end{cases} \quad (14)$$

The ninth velocity is zero which stands for the particles at rest. The length scale (1 lu) is fixed by the distance between nodes. The macroscopic density ρ, velocity $\mathbf{u}$, internal energy per unit mass e, heat flux $\mathbf{q}$, are obtained by the following relations:

$$\rho = \sum_a \tilde{f}_a, \quad (15)$$

$$\rho\mathbf{u} = \sum_a \mathbf{e}_a \tilde{f}_a, \quad (16)$$

$$\rho e = \sum_a \tilde{g}_a - \frac{\Delta t}{2}\sum_a f_a h_a, \quad (17)$$

$$\mathbf{q} = \left(\sum_a \mathbf{e}_a \tilde{g}_a - \rho e\mathbf{u} - \frac{\Delta t}{2}\sum_a \mathbf{e}_a f_a h_a\right). \quad (18)$$

Kinematic viscosity is given by $\nu = \tau_p RT_0$, and thermal diffusivity is given by $\chi = 2\tau_g RT_0$ and internal energy is related to temperature by $\rho e = \rho RT$ in 2D.

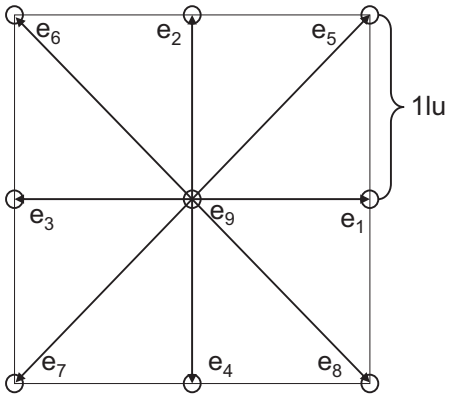

Fig. 1. The D2Q9 lattice structure.

2.1. Relation of τ with the Knudsen number

In order to simulate microscale flows with TLBM, the first step is to define the relation between Kn and the relaxation times, τ_f and τ_g. From kinetic theory, it is known that, the kinematic viscosity is $\nu = 0.5\bar{c}\lambda$ where the mean molecule velocity is $\bar{c} = \sqrt{8RT/\pi}$. Using the definition of Knudsen number, $Kn = \lambda/H$, and the expression of kinematic viscosity, Tian et al. showed that

$$Kn = \sqrt{\frac{\pi}{6}}\frac{\tau}{H\Delta t} = 0.7236\frac{\tau}{H\Delta t}. \tag{19}$$

Using the collision frequency in kinetic theory, Niu et al. [34] used the relation $\tau = \lambda/\langle v\rangle$ where the mean thermal velocity $\langle v\rangle = \sqrt{8RT/\pi}$. This gives $\tau = \sqrt{8RT/\pi}/\lambda$ and since in LBM $c = \sqrt{3RT} = 1$ for the D2Q9 model, then the relation between τ and Kn can be given as

$$Kn = \sqrt{\frac{8}{3\pi}}\frac{\tau}{H} = 0.9213\frac{\tau}{H}. \tag{20}$$

In their earlier work however, Niu et al. [33] have derived the Kn-τ relation using the Knudsen number relation with Mach number and Reynolds number given as $Kn = \sqrt{\frac{\pi\gamma}{2}}\frac{Ma}{Re}$ where $Ma = U_\infty/c_s$ and $Re = U_\infty v/H$. Since sound speed in LBM is given as $c_s = c/\sqrt{3} = 1/\sqrt{3}$, the combination with $\tau = \frac{\nu}{c_s^2}$ gives

$$Kn = \sqrt{\frac{\gamma\pi}{6}}\frac{\tau}{H} = 0.8562\frac{\tau}{H}. \tag{21}$$

In the current work, $Kn = \tau_f/H$ is employed where $\tau_f/2\tau_g = Pr$.

2.2. Thermal LBM procedure

The solution of the TLB equations given by Eqs. (2) and (3) is carried in two steps: (a) collision and (b) streaming. The collision step calculates the right hand side of Eqs. (2) and (3) and assigns the value to buffer parameters, $\tilde{f}_a^*$ and $\tilde{g}_a^*$ by

$$\tilde{f}_a^*(\mathbf{x},t) = (1-\omega_f)\tilde{f}_a(\mathbf{x},t) + \omega_f f_a^{eq}(\mathbf{x},t), \tag{22}$$

$$\tilde{g}_a^*(\mathbf{x},t) = (1-\omega_g)\tilde{g}_a(\mathbf{x},t) + \omega_g g_a^{eq}(\mathbf{x},t) - \omega_g\tau_g f_a h_a, \tag{23}$$

where $\omega_f = \Delta t/(\tau_f + 0.5\Delta t)$ and $\omega_g = \Delta t/(\tau_g + 0.5\Delta t)$. The distribution functions at the new time level are then streamed to the neighboring nodes in the streaming step by

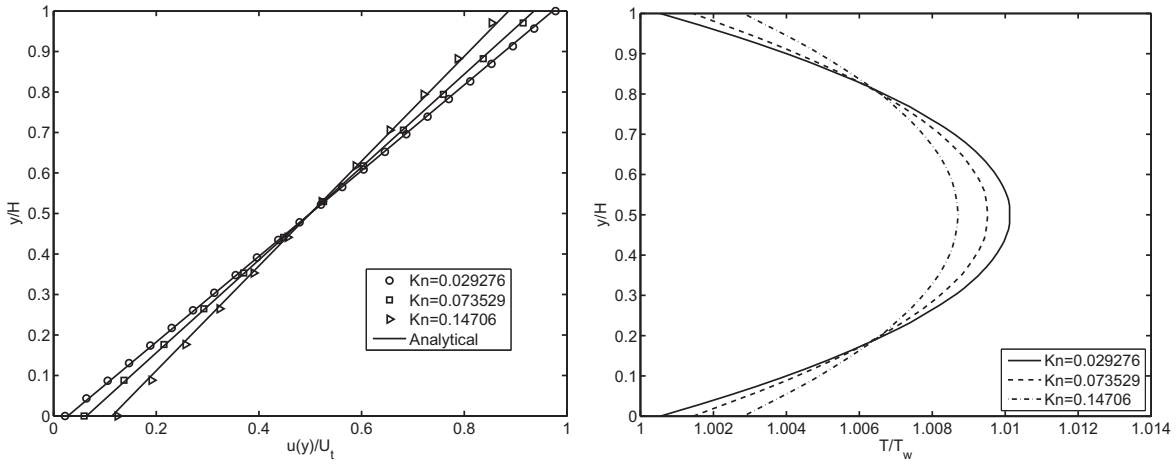

(a) Velocity profile (b) Temperature profile

Fig. 2. Cross-sectional profiles at various Kn numbers for micro-Couette flow.

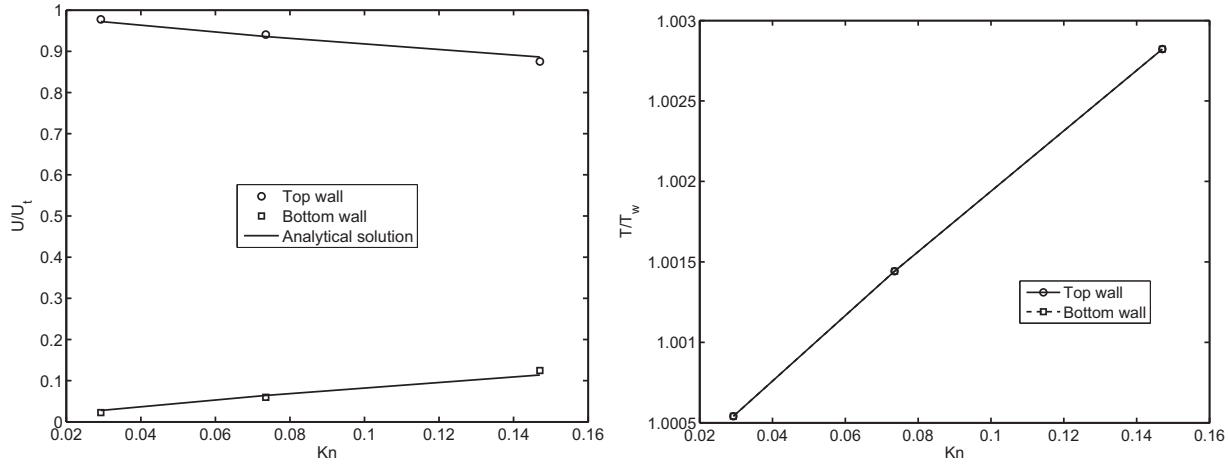

(a) Velocity slip (b) Temperature jump

Fig. 3. Effect of rarefaction on velocity slip and temperature jump for micro-Couette flow.

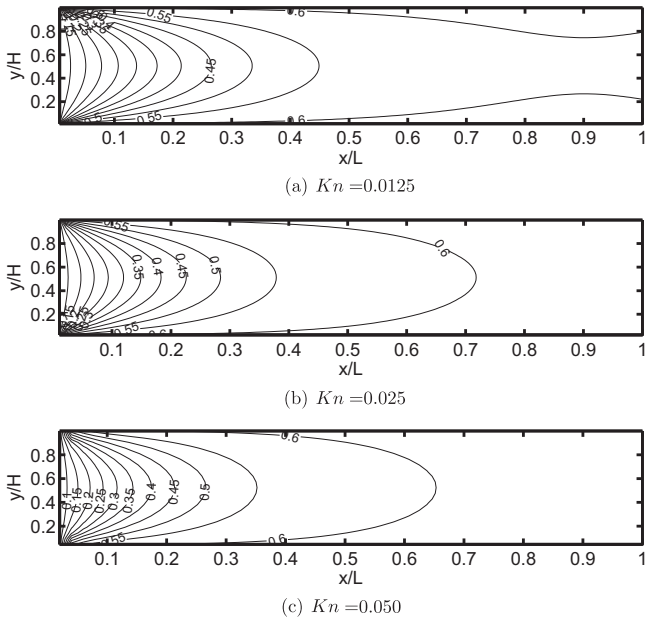

(a) Kn =0.0125

(b) Kn =0.025

(c) Kn =0.050

Fig. 4. Temperature isolines in the microchannel for various *Kn* numbers.

$$\tilde{f}_a(\mathbf{x}+\mathbf{e}_a\Delta t, t+\Delta t) = \tilde{f}_a^*(\mathbf{x}, t), \tag{24}$$

$$\tilde{g}_a(\mathbf{x}+\mathbf{e}_a\Delta t, t+\Delta t) = \tilde{g}_a^*(\mathbf{x}, t). \tag{25}$$

The LBM simulation is initialized by calculating Eqs. (10)–(13) for the equilibrium distributions $\tilde{f}_a^{eq}$ and $\tilde{g}_a^{eq}$ at all lattice nodes in the domain using the initial velocity, density and temperature values. Then the effects of boundary conditions and forces (if any) are incorporated in order to calculate the unknown buffer distributions, $\tilde{f}_a^*$ and $\tilde{g}_a^*$, at the boundaries that are directed into the flow domain. First the boundary conditions at the open ends are imposed according to the pressure and temperature values specified at inlet and outlet. Then, no-slip and constant temperature boundary conditions are applied at the walls. This is followed by the collision step where the direction-specific density distributions are relaxed toward quasi-equilibrium distributions. The equilibrium distributions are recomputed by Eqs. (10)–(13), and the particles are streamed to the neighboring nodes. Finally the macroscopic flow properties are calculated at the next time step using Eqs. (15)–(18). The pressure is related to density by $p = \rho c^2/3$ where the particle streaming speed is taken as $c = \sqrt{3RT_0}$ (assigned to 1 for now), where T_0 is the average temperature. The relation between the relaxation parameters is determined by the imposed Prandtl number, $Pr = \tau_p/\tau_g$.

2.3. Velocity and thermal boundary conditions

2.3.1. Inlet and outlet boundaries

For Couette flow and for the force driven channel flow periodic boundary conditions are applied at the inlet. For Poiseuille flow and channel flow with a blockage cases the a constant velocity and temperature profile is assigned at the inlet and at the exit the unknown distribution functions were extrapolated from the neighboring fluid nodes. To specify a constant temperature profile at the inlet boundary, the incoming unknown thermal populations $(\tilde{g}_1, \tilde{g}_5, \tilde{g}_8)$ are assumed to be equilibrium distribution functions, with e_i thermal energy density imposed at the inlet. The unknown exit thermal populations facing the flow domain are set equal to those of the nearest interior nodes. To specify the velocity at the inlet, the idea of bounce-back of non-equilibrium part of the particle distribution function proposed by Zou and He [37]. The velocity component normal to the inlet boundary is assumed to be zero and the density is to be determined. After streaming, at the inlet boundary $(\tilde{f}_1, \tilde{f}_5, \tilde{f}_8)$ are unknown. Using Eqs. (15) and (16) the density at the inlet ρ_i and unknown density functions are calculated as follows:

$$\rho_{in} = \frac{\left(\tilde{f}_9 + \tilde{f}_2 + \tilde{f}_4 + 2(\tilde{f}_3 + \tilde{f}_6 + \tilde{f}_7)\right)}{(1-u_i)}, \tag{26}$$

$$\tilde{f}_1 = \tilde{f}_3 + \frac{2}{3}\rho_{in}u_{in}, \tag{27}$$

$$\tilde{f}_5 = \tilde{f}_7 - \frac{1}{2}\left(\tilde{f}_2 - \tilde{f}_4\right) + \frac{1}{6}\rho_i u_i, \tag{28}$$

$$\tilde{f}_8 = \tilde{f}_6 + \frac{1}{2}\left(\tilde{f}_2 - \tilde{f}_4\right) + \frac{1}{6}\rho_i u_i. \tag{29}$$

In order to obtain the above equations, the bounce-back rule for the non-equilibrium part of the momentum density population normal to the inlet was used as, $\tilde{f}_1 - \tilde{f}_1^{eq} = \tilde{f}_3 - \tilde{f}_3^{eq}$.

2.3.2. Velocity slip and temperature jump boundary conditions

The critical issue in extending the TLBM into microflow simulation is the appropriate treatment of fluid solid interactions. Zhang [15] has used the second-order slip model of Cercignani in their isothermal LBM simulations whereas Tian et al. [36] has applied it to TLBM for $Kn < 0.1$ where the second order terms were assumed to be negligible. Here we use the first-order slip boundary condition given as

$$u_{y=0}^{slip} = u_{y=0} - u_{wall} = \sigma Kn\left(\frac{\partial u}{\partial y}\right)_{y=0}, \tag{30}$$

$$u_{y=H}^{slip} = u_{wall} - u_{y=H} = \sigma Kn\left(\frac{\partial u}{\partial y}\right)_{y=H}, \tag{31}$$

$$T_{y=0}^{jump} = T_{y=0} - T_{wall} = \alpha\left(\frac{2\gamma}{\gamma+1}\right)\left(\frac{Kn}{Pr}\right)\left(\frac{\partial T}{\partial y}\right)_{y=0}, \tag{32}$$

$$T_{y=H}^{jump} = T_{wall} - T_{y=H} = \alpha\left(\frac{2\gamma}{\gamma+1}\right)\left(\frac{Kn}{Pr}\right)\left(\frac{\partial T}{\partial y}\right)_{y=H}, \tag{33}$$

where $\sigma = (2-\sigma_v)/\sigma_v$ and $\alpha = (2-\alpha_T)/\alpha_T$. The tangential momentum accommodation coefficient σ_v is defined as the fraction of molecules reflected diffusively from the wall, and α_T is the thermal accommodation coefficient. Both coefficients are generally assigned to one which means that the molecules hitting the wall boundary are reflected back completely diffusively which means that they forget the information before the collision and take on the values of the wall after the collision. The above equations are reorganized to get the velocity and temperature values at the walls as

$$u_{y=0} = Kn\left(\frac{4u_1 - u_2}{2\Delta x + 3Kn}\right), \tag{34}$$

$$u_{y=H} = \frac{(Kn(4u_{H-1} - u_{H-2}) + 2\Delta x U_H)}{2\Delta x + 3Kn}, \tag{35}$$

$$T_{y=0} = \frac{(C_{jump}Kn(4T_1 - T_2) + 2\Delta x T_0)}{2\Delta x + 3C_{jump}Kn}, \tag{36}$$

$$T_{y=H} = \frac{(C_{jump}Kn(4T_{H-1} - T_{H-2}) + 2\Delta x T_H)}{2\Delta x + 3C_{jump}Kn}, \tag{37}$$

where $C_{jump} = \alpha(2\gamma\ (\gamma+1)Pr)$ and second order implicit finite-difference scheme is used to obtain the derivatives.

3. Results

3.1. Thermal micro-Couette flow

Micro-Couette flow with zero temperature gradient was solved using the TLBM. The flow is driven by the top wall moving at U_t while the temperature of both walls is kept same $(T_t = T_b)$. Periodic boundary conditions for both velocity and energy distributions

were applied at the open boundaries. Air's properties at room temperature are used here for $\gamma = 1.4$ and $Pr = 0.7$. Density and temperature variations along the axial direction are negligible. Initially, the flow is at rest with temperature equal to the wall temperature. Fig. 2 show the linear velocity profile and nonlinear temperature profiles respectively with *Kn* varying from 0.12 to 0.48. The temperature jump is observed to increase with the Knudsen number increasing. The reduction in wall velocity and increase in temperature is plotted in Fig. 3.

3.2. Thermal micro-Poiseuille flow

A 2D planar microchannel flow driven by a constant inlet velocity profile U_i, with the walls at rest and at constant temperature

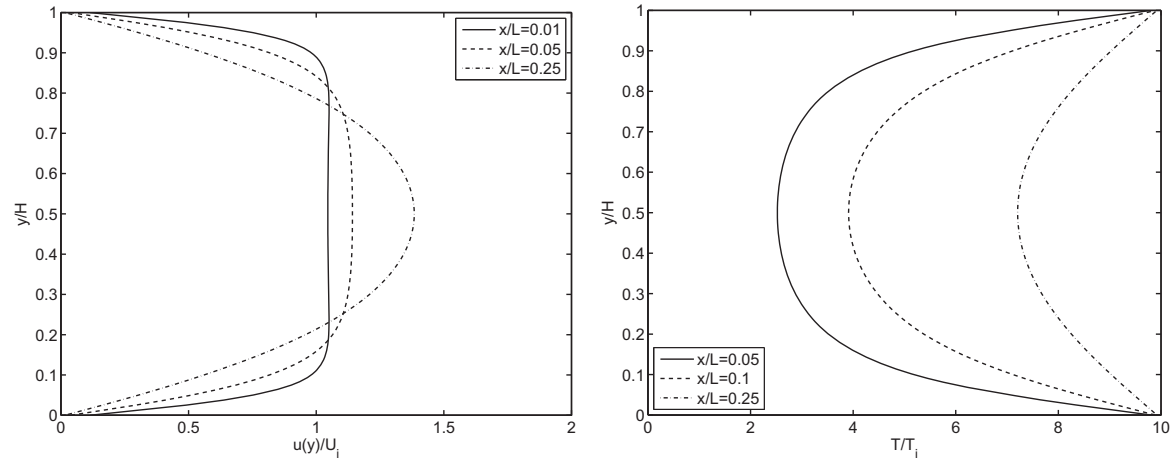

(a) Kn =0.0125

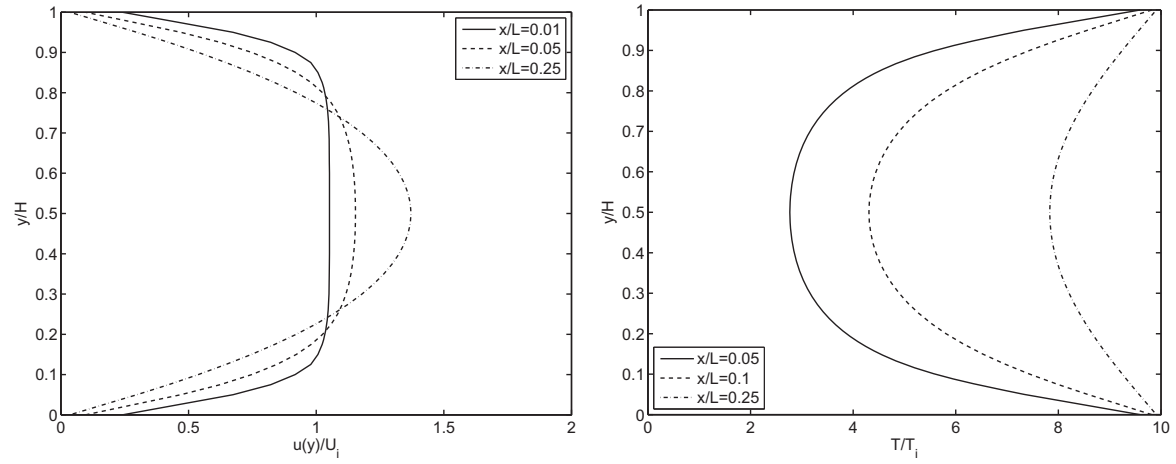

(b) Kn =0.025

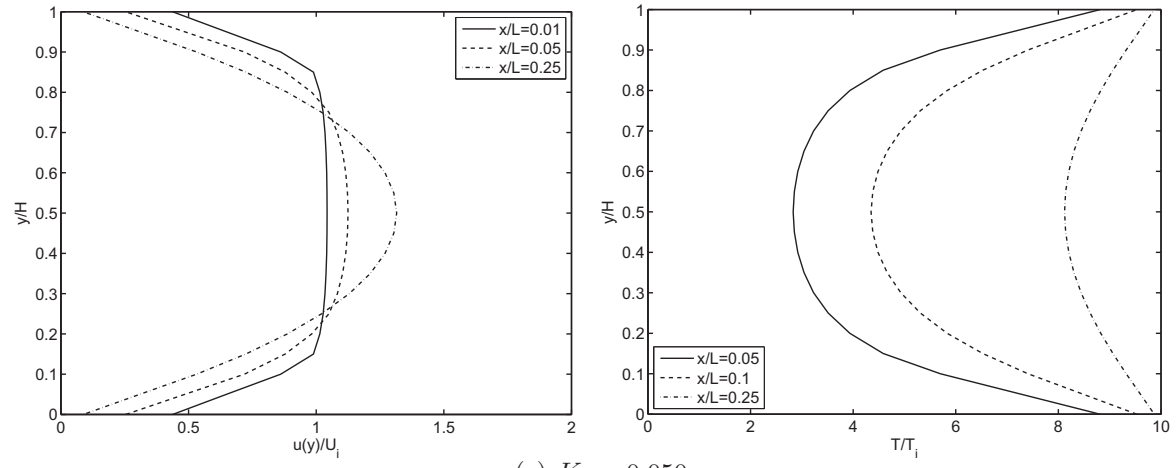

(c) Kn =0.050

Fig. 5. Velocity profiles along the microchannel at various *Kn* numbers.

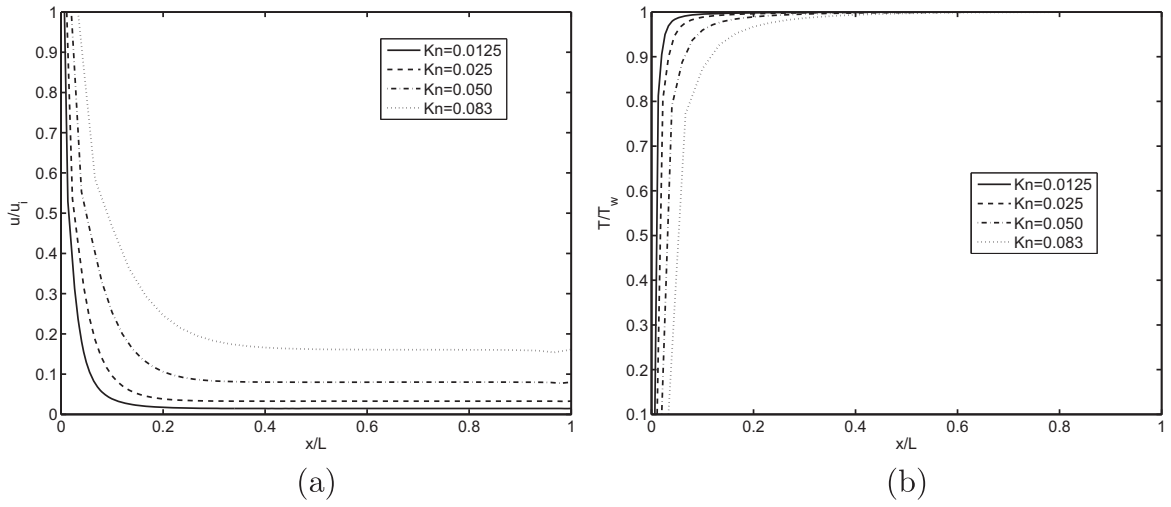

Fig. 6. Velocity slip (a) and wall temperature jump (b) variation along the thermally developing channel.

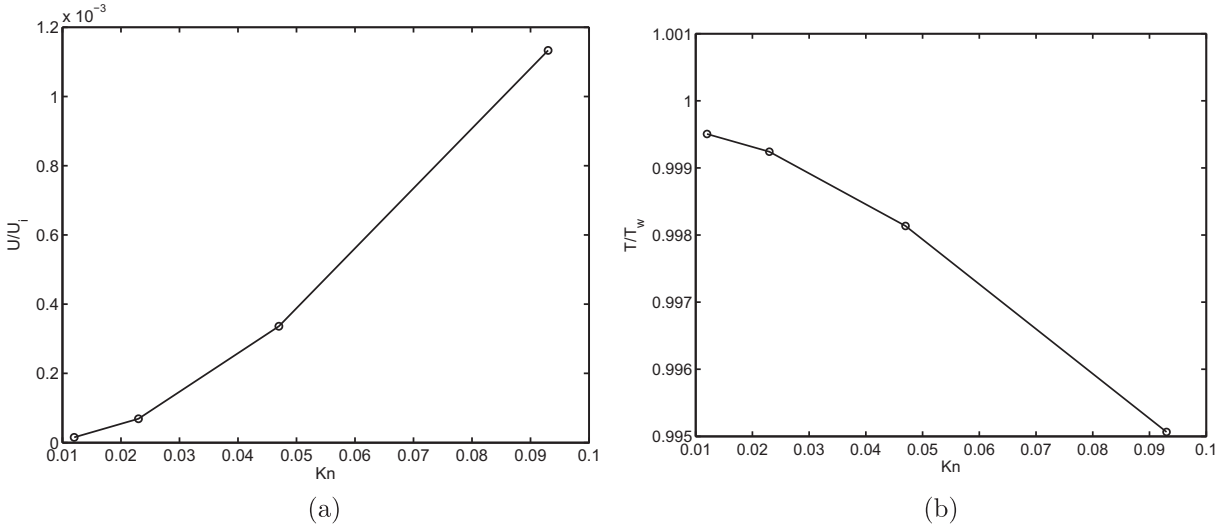

Fig. 7. Effect of *Kn* number on velocity slip (a) and wall temperature jump.

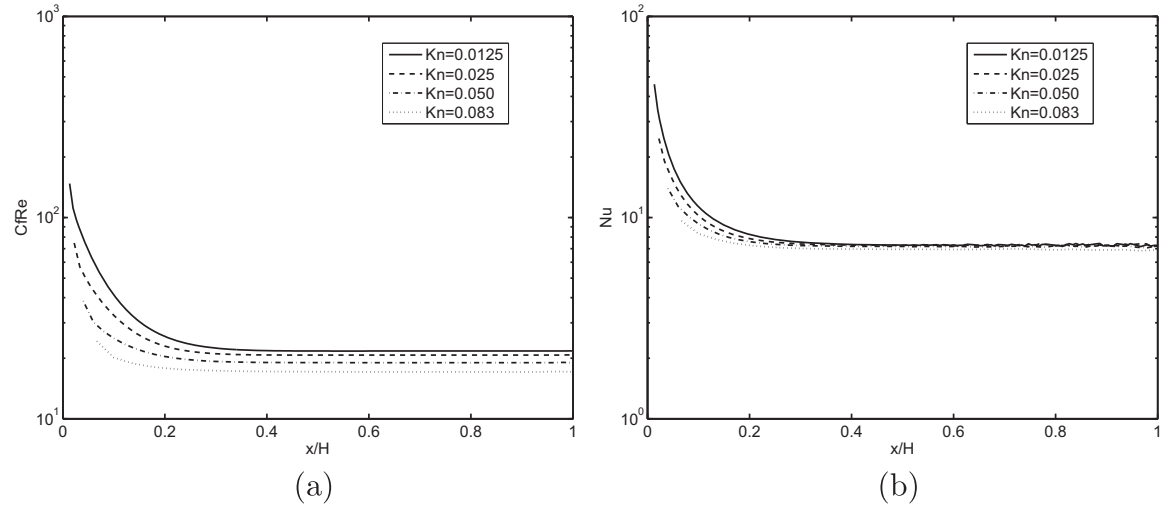

Fig. 8. Local skin friction coefficient (a) and local Nusselt number (b) variation along the thermally developing channel.

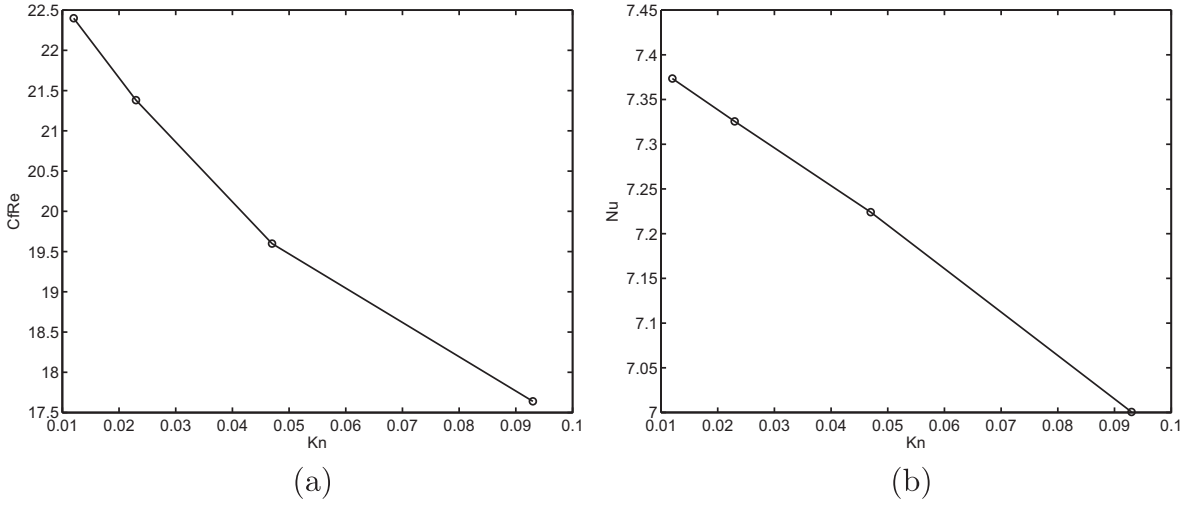

Fig. 9. Outlet local skin friction coefficient (a) and local Nusselt number (b) variation with Kn number.

$T_t = T_b$, is considered. The walls are kept at constant temperatures and the channel is cooled at the inlet, $10T_i = T_t = T_b$. The temperature contours at $Kn = 0.0125 - 0.05$ are shown in Fig. 4. It is observed that the rarefaction effect reduces the convection from the cooler inlet stream. The velocity slip and temperature jump can be observed in Fig. 5 by comparing velocity and temperature profiles along the microchannel for $Kn = 0.0125 - 0.05$.

The axial variation of the amount of velocity slip and temperature jump is presented in Fig. 6. In the developing region, the velocity and temperature values at the wall are higher in the slip regime compared to the continuum regime. This is still valid for velocity in the developed region however the temperature value approaches to the wall temperature and Kn does not seem to affect the temperature distribution so much in the developed region. However, the outlet slip and temperature values at the wall tend to change nonlinearly as the rarefaction is increased. Fig. 7 shows this effect where the wall velocity approaches to zero for $Kn \to 0$ and temperature value approaches to wall temperature. In Fig. 8 the variation of local skin friction coefficient and Nusselt number is plotted for $Kn = 0.0125 - 0.083$. It can be seen that the increase of Knudsen number causes the friction coefficient and Nusselt number decreased. Near the entrance region where the flow is developing very fast, the Knudsen number has a great effect on the friction coefficient and Nusselt number. The outlet $CfRe$ and Nu are observed to decrease as Kn is increased as shown in Fig. 9 which is in agreement with previous data in literature [14]. The values for $CfRe$ and Nu approach to their continuum values as the $Kn \to 0$.

4. Conclusions

In this paper the TLBM computations of incompressible flow and heat transfer in microchannels have been reported. The relaxation parameter is related to the Knudsen number and Maxwell's slip boundary treatment is used to calculate the velocity and temperature values at the wall boundaries. Thermal micro-Couette and thermal micro-Poiseuille flow in a straight channel are simulated as test cases. It is observed that the present method can model the microscale flow and heat transfer characteristics.

Conflict of interest

None declared.

References

[1] X. Nie, G.D. Doolen, S. Chen, Lattice-Boltzmann simulations of fluid flow in MEMS, J. Stat. Phys. 107 (2002) 279–289.
[2] C. Lim, C. Shu, X. Niu, Y. Chew, Application of lattice Boltzmann method to simulate microchannel flows, Phys. Fluids 14 (7) (2002) 2299–2308.
[3] E. Arkilic, M. Schmidt, K. Breuer, Gaseous slip flow in long microchannels, J. Microelectromech. Syst. 6 (2) (1997) 167–178.
[4] K.-C. Pong, C.-M. Ho, J. Liu, Y.-C. Tai, Non-linear Pressure Distribution in Uniform Microchannels, 197, American Society of Mechanical Engineers, Fluids Engineering Division (Publication) FED, 1994. 51–56.
[5] G. Tang, W. Tao, Y. He, Gas flow study in MEMS using lattice Boltzmann method, Int. Conf. Microchannels Minichannels 1 (2003) 389–396.
[6] C.Y. Lim, C. Shu, X.D. Niu, Y.Y. Chew, Application of lattice Boltzmann method to simulate microchannel flows, Phys. Fluids 14 (7) (2002) 2299.
[7] J.C. Shih, C.-M. Ho, J. Liu, Y.-C. Tai, Monatomic and Polyatomic Gas Flow Through Uniform Microchannels, 59, American Society of Mechanical Engineers, Dynamic Systems and Control Division (Publication) DSC, 1996. 197–203.
[8] G. Tang, W. Tao, Y. He, Three-dimensional lattice Boltzmann model for gaseous flow in rectangular microducts and microscale porous media, J. Appl. Phys. 97 (10) (2005) 104918.
[9] C. Aubert, S. Colin, High-order boundary conditions for gaseous flows in rectangular microducts, Microscale Thermophys. Eng. 5 (1) (2001) 41–54.
[10] C. Shen, D. Tian, C. Xie, J. Fan, Examination of the LBM in simulation of microchannel flow in transitional regime, Microscale Thermophys. Eng. 8 (4) (2004) 423–432.
[11] S. Chen, D. Martinez, R. Mei, On boundary conditions in lattice Boltzmann methods, Phys. Fluids 8 (9) (1996) 2527.
[12] T. Lee, C.-L. Lin, Rarefaction and compressibility effects of the lattice-Boltzmann-equation method in a gas microchannel 71 (4) (2005) 046706-1. URLhttp://dx.doi.org/10.1103/PhysRevE.71.046706.
[13] T. Ohwada, Y. Sone, K. Aoki, Numerical analysis of the Poiseuille and thermal transpiration flows between two parallel plates on the basis of the Boltzmann equation for hard-sphere molecules, Phys. Fluids A: Fluid Dyn. 1 (1989) 2042–2049.
[14] G. Karniadakis, A. Beskok, Micro Flows: Fundamentals and Simulation, Springer-Verlag, NY, U.S.A, 2001.
[15] Y. Zhang, R. Qin, R. Emerson, David, Lattice Boltzmann simulation of rarefied gas flows in microchannels, Phys. Rev. E Stat. Nonlinear Soft Matter Phys. 71 (4) (2005) 047702. URL http://dx.doi.org/10.1103/PhysRevE.71.047702.
[16] S. Tison, Experimental data and theoretical modeling of gas flows through metal capillary leaks, Vacuum 44 (11–12) (1993) 1171–1175.
[17] F. Toschi, S. Succi, Lattice Boltzmann method at finite Knudsen numbers, Europhys. Lett. 69 (4) (2005) 549–555.
[18] S. Ansumali, I.V. Karlin, Kinetic boundary conditions in the lattice Boltzmann method, Phys. Rev. E 66 (2) (2002) 026311–026317.
[19] C. Cercignani, M. Lampis, S. Lorenzani, Variational approach to gas flows in microchannels, Phys. Fluids 16 (9) (2004) 3426–3437.
[20] Y. Zhou, R. Zhang, I. Staroselsky, H. Chen, W. Kim, M. Jhon, Simulation of micro- and nano-scale flows via the lattice Boltzmann method, Physica A 362 (1) (2006) 68–77.
[21] S. Chen, G.D. Doolen, Lattice Boltzmann method for fluid flows, Annu. Rev. Fluid Mech. 30 (1998) 329–364.
[22] R. Benzi, S. Succi, M. Vergassola, The lattice Boltzmann equation: theory and applications, Phys. Rep. 222 (3) (1992) 145–197.

[23] Y. Peng, C. Shu, Y.T. Chew, Simplified thermal lattice Boltzmann model for incompressible thermal flows, Phys. Rev. E 68 (2) (2003) 026701.
[24] A. D'Orazio, M. Corcione, G.P. Celata, Application to natural convection enclosed flows of a lattice Boltzmann BGK model coupled with a general purpose thermal boundary condition, Int. J. Therm. Sci. 43 (6) (2004) 575–586.
[25] X. He, S. Chen, G.D. Doolen, A novel thermal model for the lattice Boltzmann method in incompressible limit, J. Comput. Phys. 146 (1) (1998) 282–300.
[26] H.N. Dixit, V. Babu, Simulation of high Rayleigh number natural convection in a square cavity using the lattice Boltzmann method, Int. J. Heat Mass Transfer 49 (2006) 727–739.
[27] G.H. Tang, W.Q. Tao, Y.L. He, Thermal boundary condition for the thermal lattice Boltzmann equation, Phys. Rev. E 72 (1) (2005) 016703–+.
[28] A. D'Orazio, S. Succi, Simulating two-dimensional thermal channel flows by means of a lattice Boltzmann method with new boundary conditions, Future Gener. Comput. Syst. 20 (2004) 935–944.
[29] H. Huang, T.S. Lee, C. Shu, Thermal curved boundary treatment for the thermal lattice Boltzmann equation, Int. J. Mod. Phys. C 17 (2006) 631–643.
[30] Z. Guo, C. Zheng, B. Shi, An extrapolation method for boundary conditions in lattice Boltzmann method, Phys. Fluids 14 (6) (2002) 2007–2010.
[31] C.-K. Chen, T.-S. Yen, Y.-T. Yang, Lattice Boltzmann method simulation of backward-facing step flow with double plates aligned at angle to flow direction, J. Heat Transfer 128 (11) (2006) 1176–1184.
[32] S. Gokaltun, S.G. Dulikravich, Lattice Boltzmann simulations for flow and heat transfer in constricted channels, Comput. Math. Appl. 59 (7) (2010) 2431–2441.
[33] C. Shu, X.D. Niu, Y.T. Chew, A lattice Boltzmann kinetic model for microflow and heat transfer, J. Stat. Phys. 121 (1–2) (2005) 239–255.
[34] X.D. Niu, C. Shu, Y.T. Chew, A thermal lattice Boltzmann model with diffuse scattering boundary condition for micro thermal flows, Comput. Fluids 36 (2007) 273–281.
[35] C.H. Wang, R. Yang, A numerical study for slip flow heat transfer, Appl. Math. Comput. 173 (2) (2006) 1246–1264.
[36] Z.W. Tian, C. Zou, Z.H. Liu, Z.L. Guo, H.J. Liu, C.G. Zheng, Lattice Boltzmann method in simulation of thermal micro-flow with temperature jump, Int. J. Mod. Phys. C 17 (5) (2006) 603–614.
[37] Q. Zou, X. He, On pressure and velocity boundary conditions for the lattice Boltzmann BGK model, Phys. Fluids 9 (6) (1997) 1591–1598.